PHYSIC WITH POLARIZED PARTICLES

V. W. Hughes

Yale University, New Haven, Connecticut (USA)

A - INTRODUCTION: INFORMATION FROM STUDIES WITH POLARIZED PARTICLES

I shall try to review the status of high energy physics with polarized particles. Physics experiments at high energies with polarized particles are beginning to be done. Targets of polarized protons have been used in studies of pion-proton and proton-proton scattering and there are experiments in progress to determine the parities of elementary particles. As yet accelerated beams of polarized particles have not been used in high energy experiments, but many nuclear physics experiments have been done with polarized beams from lower energy accelerators (1, 2).

Some of the types of information available from studies with polarized particles are indicated in Table I. There has been relatively little theoretical discussion of polarization phenomena in high energy physics, presumably largely due to the scarcity of experimental information.

As regards the symmetries and general properties of interactions, it is well known that spin polarization plays an important role in the study of the invariance properties of interactions. An interaction term of the form $\vec{\sigma} \cdot \vec{p}$ indicates violation of parity conservation, in which $\vec{\sigma}$ is the spin or intrinsic angular momentum operator and $\vec{p}$ is the linear momentum operator (3). At present the primary evidence on parity conservation in the strong interactions comes from low energy nuclear physics experiments, principally from studies of the electromagnetic decays of excited nuclear states (4) but also from a nuclear reaction experiment using a polarized deuteron beam (5).

Time reversal invariance in the strong interactions can be tested by comparing the polarization, P, of the recoil proton produced in the elastic scattering of unpolarized protons from a target of unpolarized protons with the left-right asymmetry, P', produced in the elastic scattering of unpolarized protons from a target of polarized protons. If both of these scattering experiments are performed at the same energy and scattering angle, time reversal invariance requires (6) that $P = P'$. A significant experiment based on this principle has been performed (7) for protons in the energy range of 140 to 210 MeV. Te equality in differential cross section of a reaction and of the inverse reaction for more complex nuclear reactions, such as $\alpha + C^{12} \leftrightarrows N^{14} + d$, also can serve as a test of time reversal invariance, and indeed several of the most sensitive tests for T invariance come from such studies done in the 10 to 40 MeV range (8).

Tests of the general properties of scattering amplitudes such as dispersion relations and asymptotic high energy limits generally require in principle that the spin dependent part of the scattering amplitude be known (9, 10). For the description of the elastic scattering of a spin 0 particle by a spin 1/2 particle, under the assumptions of space reflection invariance and time reversal invariance, two invariant complex

TABLE I

Types of information from studies with polarized particles

I. Symmetries and General Properties of Interactions
   1. P. invariance
   2. T invariance
   3. Tests of dispersion relations
   4. Asymptotic high energy limits of scattering amplitudes.

II. Specific spin dependence of particle interactions
   1. Complete determination of scattering matrices
      a) Elastic
      b) Inelastic
   2. Nucleon-nucleon interaction
   3. Pion-nucleon interaction
   4. Electron-proton and electron-deuteron scattering
      a) Validity of Rosenbluth formula
      b) Spin-flip pion production cross section in hydrogen
      c) Deuteron electric quadrupole form factor
   5. Photodisintegration (deuteron)

III. Properties of particles or resonant states
   1. Spin
   2. Parity

amplitudes are needed, one of which involves the spin operator. For the description of the scattering of two identical spin 1/2 particles, five complex amplitudes are needed, three of which involve the spin operators. For small angle scattering the elastic scattering of a spin zero particle by a spin 1/2 particcle can probably be approximated well with a single spin independent complex amplitude, but for the elastic scattering of two identical spin 1/2 particles no such approximation is justified. Hence in general, since spin dependent amplitudes, where measured, are of appreciable magnitude, it is clear that a knowledge of these amplitudes will be required for critical tests of the general properties of scattering amplitudes.

The complete determination of scattering matrices requires experiments with polarized particles. With the assumptions of space reflection invariance and time reversal invariance the scattering matrix for an elastic collision between a spin 0 and a spin 1/2 particle in the barycentric system can be written (9):

$$T(\vec{K}_f, \vec{K}, \vec{\sigma}) = f\,\vec{1} + ig\,\vec{\sigma}\cdot\vec{K}\times\vec{K}_f$$

in wich $\vec{\sigma}$ is the Pauli spin operator, $\vec{K}$ is the three momentum of the incident particle, $\vec{K}_f$ is the final momentum and 1 is a unit 2×2 matrix. The functions f and g may be complex and are functions of energy and scattering angle. Since a simple scattering experiment to measure the differential scattering cross section, $d\sigma/d\Omega$, can only determine one relation between these functions, experiments with polarized beams or targets are required to provide the additional relationships needed for the complete determination of the scattering matrix. The most common example for the spin 0 particle and spin 1/2 particle system is the pion-proton system.

Analogously, with the assumptions of space reflection invariance and time reversal invariance the scattering matrix for an elastic collision between two identical spin 1/2 particles (e.g. proton-proton scattering) can be written:

$$T(\vec{K}_f, \vec{K}, \vec{\sigma_1}, \vec{\sigma_2}) = \alpha + \beta(\vec{\sigma_1}\cdot\hat{n})(\vec{\sigma_2}\cdot\hat{n}) + i\gamma(\vec{\sigma_1}+\vec{\sigma_2})\cdot\hat{n} + \delta(\vec{\sigma_1}\cdot\hat{m})(\vec{\sigma_2}\cdot\hat{m}) + \varepsilon(\vec{\sigma_1}\cdot\vec{l})(\vec{\sigma_2}\cdot\vec{l})$$

in which

$$\vec{l} = \frac{\hat{K}+\hat{K}_f}{2\cos(\theta/2)},\quad m = \frac{\hat{K}-\hat{K}_f}{2\sin\theta/2},\quad \hat{n} = \frac{\hat{K}\times\hat{K}_f}{\sin\theta}$$

where θ is the angle between $\hat{K}$ and $\hat{K}_f$. The quantitaties α, β, γ, δ, ε are complex functions of energy and scattering angle.

In the energy range up to the threshold for pion production there has been extensive experimental and theoretical work on proton-proton and proton-neutron scattering (here noniden-

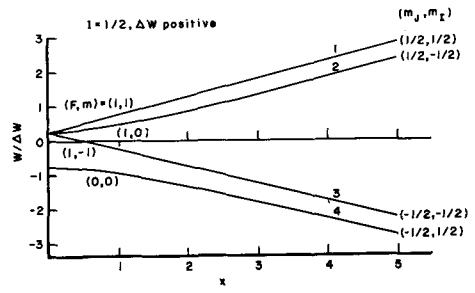

Fig. 1 - Energy level diagram for hydrogen in a magnetic field H, obtained from the Breit-Rabi equation:

$$W_{F=I\pm 1/2,m} = -\frac{\Delta W}{2(2I+1)} + \mu_o g_I H m \pm \frac{\Delta W}{2}\left[1+\frac{4mx}{2I+1}+x^2\right]^{1/2}$$

ΔW is the zero field hfs separation between the states $F = I + 1/2$ and $F = I - 1/2$ [$\Delta W = W_{I+1/2}(H=0) - W_{I-1/2}(H=0)$];
$x = (g_J - g_I)\,\mu_o H/\Delta W$; g_J and g_I are the electronic and nuclear g-values in units in which $g_J \simeq 2$; μ_o = Bohr magneton. For hydrogen, $J = 1/2$, $I = 1/2$, $\Delta W/h = \Delta\nu = 1420.4$ Mc/s, $g_J = 2.002$, $g_I = -0.0030$. The levels are designated by both their weak field quantum numbers (F, m) and their strong field quantum numbers (m_J, m_I). For convenience of the discussion the four levels are designated by the numbers 1, 2, 3, and 4.

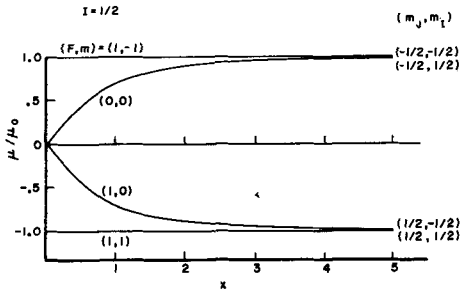

Fig. 2 - The magnetic moments of the magnetic sublevels of the hfs states of hydrogen with $J = 1/2$ and $I = 1/2$ as a function of magnetic field H, obtained from the equation:

$$\frac{\mu_{F=I+1/2,m}}{\mu_o} = -\frac{1}{\mu_o}\frac{\partial W_{F,m}}{\partial H} = -g_I m \pm \frac{x/2 + m/(2I+1)}{[1+4mx/(2I+1)+x^2]^{1/2}}(g_J - g_I)$$

for $m = I - 1/2,\ I - 3/2, \ldots, -(I-1/2)$.

$$\frac{\mu_{F=I+1/2,m=\pm(I+1/2)}}{\mu_o} = \mp(g_J/2 + g_I I)$$

The levels are designated by both their weak field quantum numbers (F,m) and their strong field quantum numbers (m_J, m_I).

tical particles are involved and six complex functions are needed) to determine the phase shifts which define the scattering matrix (11). Double and triple scattering experiments which determine polarization and spin correlation functions have been performed and analyzed. At higher energies up to the multi-BeV range measurements of total cross sections, differential cross sections, and of a polarization parameter have been made (12). Although the results suggest that the principal scattering amplitude has an appreciable real part, which is a point of considerable

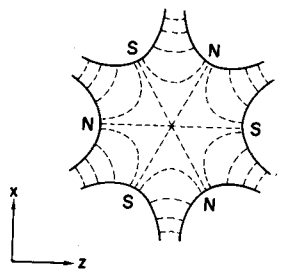

Fig. 3 - Field and potential lines for a magnetic field which varies as the square of the distance from the axis. Field lines are dashed (— — — —); potential lines are solid (—); axis is through the geometrical center of diagram perpendicular to figure. The force on an atom acts in the radial direction.

interest, lack of information about the spin dependent amplitudes leaves the matter somewhat ambiguous (10).

The scattering matrices for inelastic processes will, of course, also involve spin dependent functions. Very little work at high energies has yet been done on these more complicated problems.

For elastic electron-proton scattering the use of polarized electrons in conjunction with a polarized proton target or with a measurement of the polarization of the recoil proton or scattered electron would allow determinations of different combinations of the Dirac and Pauli form factors than are determined in elastic scattering with unpolarized particles and would also permit a test of the validity of the Rosenbluth formula (13).

For elastic scattering the use of a polarized electron beam together with a polarized deuteron target would allow a separate determination of the charge, quadropole and magnetic form factors (14). More generally the combination of a polarized electron beam and a polarized nuclear target would allow the determination of nuclear quadrupole form factors.

Inelastic single pion production in the spin-flip scattering of polarized electrons by polarized protons would be a very difficult experiment, but it might elucidate (15) the outstanding discrepancy between the experimental and theoretical values of the hyperfine structure interval for hydrogen (16).

The study of the photodisintegration of the deuteron using polarized deuteron targets, and possibly circularly polarized bremsstrahlung, would aid in the determination of the proton-neutron interaction (17).

The parities of strange particles may be determined from the left-right asymmetry in production reactions involving polarized proton targets. Thus a study of the reactions

$$\pi^- + p \rightarrow \Lambda^\circ + K^\circ$$

$$\pi^+ + p \rightarrow \Sigma^+ + K^+$$

can yield the relative parities or the Λ and Σ particles (18). An experiment using a polarized proton target has been proposed to test the parity of the Ω^- particle (19).

Through measurements of the differential cross sections and polarization parameters for scattering at energies in the neighborhood of resonant states the spins of these resonant states may be determined (20).

In bremsstrahlung longitudinally polarized electrons will produce circularly polarized gamma rays, which in turn might be used in a photoproduction experiment with a polarized proton target to measure the spins and parities of resonant states by observing the angular distribution of the decay products (21).

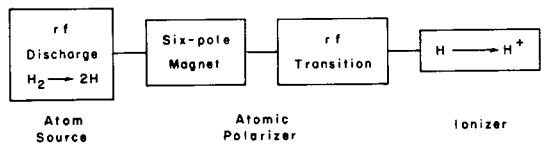

Fig. 4 - Schematic diagram of polarized ion source.

B - POLARIZED BEAMS

1. Source of polarized nuclei

Although no high energy experiment has yet been done with an accelerated beam of polarized particles, sources of polarized protons, deuterons and electrons are now available, and acceleration of polarized particles to high energies should be possible. Many experiments in nuclear physics have been done with accelerated beams of polarized protons and deuterons using electrostatic accelerators (both single-ended and tandem), cyclotrons, and linear accelerators (1, 2, 22). The highest energy accelerated beams

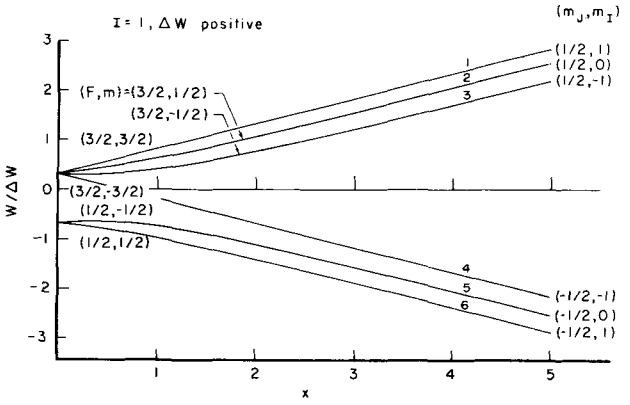

Fig. 5 - Energy level diagram for deuterium in a magnetic field H, obtained from the Breit-Rabi equation as given in caption to Fig. 1. For deuterium, $J = 1/2$, $I = 1$, $\Delta\nu = 327.38$ Mc/s, $g_J = 2.002$, and $g_I = -0.00047$. Further description is the same as for Fig. 1. The six levels are designated by the numbers 1, 2, 3, 4, 5, and 6.

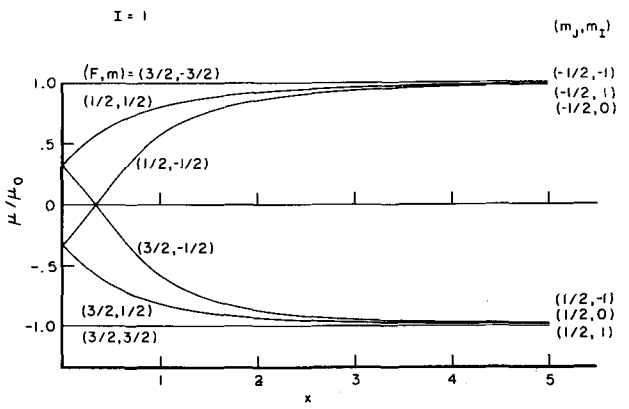

Fig. 6 - The magnetic moments of the magnetic sublevels of the hfs states of deuterium with $J = 1/2$, and $I = 1$ as a function of magnetic field H, obtained from the equations given in the caption to Fig. 2. Further description is the same as for Fig. 2.

used thus far are 50 to 60 MeV and they have been obtained with proton linear accelerators.

Successful sources have all been based on atomic beam techniques (23). Polarized atoms of thermal velocity are selected by deflection in a static inhomogeneous magnetic field (Stern-Gerlach effect). Higher nuclear polarization for the atoms can then be obtained by the use of an f.r. transition (24, 25). The polarized atoms are ionized by electron bombardment to yield polarized nuclei which can serve as the ion source for an accelerator.

A more detailed discussion of the technique is now given for a polarized proton source. The energy level diagram (26) for the ground state of the hydrogen atom in a magnetic field is shown in Fig. 1. At zero magnetic field there are the two hyperfine structure levels corresponding to values of the total angular momentum quantum number, F, equal to 1 (triplet state) and 0 (singlet state). In the presence of a magnetic field H the three degenerate magnetic sublevels of the $F = 1$ state ($m = +1, 0, -1$ are split by the Zeeman effect. At strong magnetic fields, where the interaction of the external magnetic field with the electronic magnetic moment is large compared to the hyperfine structure interaction, the atomic energy levels are described by the strong field quantum numbers m_J, the electronic magnetic quantum number, and m_I, the proton magnetic quantum number. The atomic magnetic moments of the four hyperfine structure states as a function of magnetic field are shown in Fig. 2. At strong fields the two states with $m_J = -1/2$ have a magnetic moment of $+\mu_0$, the Bohr magneton, whereas the two states with $m_J = +1/2$ have a magnetic moment of $-\mu_0$.

The selection of atoms in the two states with $m_J = +1/2$ is done by deflection in a strong inhomogeneous static magnetic field. Usually a six-pole magnetic field is employed, with the field configuration shown in Fig. 3. An atom experiences a force in a magnetic field given by

$$\vec{F} = -\frac{\partial W}{\partial H}\frac{\partial H}{\partial \vec{r}} \qquad \mu = -\frac{\partial W}{\partial H}$$

in which W(H) is the energy of the atom. For a six-pole magnet the magnitude of the field is given by

$$H = H_0 (r/a)^2$$

in which r is the radial distance from the axis in cylindrical coordinates, a is the radial distance to a pole tip, and H_0 is the field at the pole tip. Hence the force will be

$$\vec{F} = \frac{2H_0}{a^2}\mu\,\vec{r}.$$

An atom with a negative atomic magnetic moment μ will execute simple harmonic motion and be transmitted through the magnet. On the other hand, an atom with a positive atomic magnetic moment will experience a force which is directed radially outward and will strike the poles of the magnet. The efficiency of the magnet in transmitting only atoms with $m_J = +1/2$ is easily made greater than 95% if the magnet is sufficiently long.

The nuclear (proton) polarization, $P = \langle I_z \rangle / I$, of a beam having equal populations in states 1 and 2 will be zero at strong field and 1/2 at zero

field. Hence if the beam from the six-pole field enters an ionization region having a weak magnetic field and if the atoms change adiabatically from their high field states to the corresponding low field states, as usually occurs in practice because of the low velocity of the atoms, then ionization of the beam will lead to a proton polarization of about 1/2.

A radiofrequency transition can be used to increase the polarization of the protons either by the adiabatic passage method (24) or by a simple induced transition which is commonly employed in atomic beam radiofrequency spectroscopy (25, 26). With either method a transition of atoms from state 2 to state 4 can be achieved (See Fig. 1). The adiabatic method has the advantage that all atoms in state 2 can be transferred to state 4, whereas the simple induced transition can transfer at most a fraction 0,76 of the atoms due to the velocity distribution in the atomic beam. On the other hand, smaller

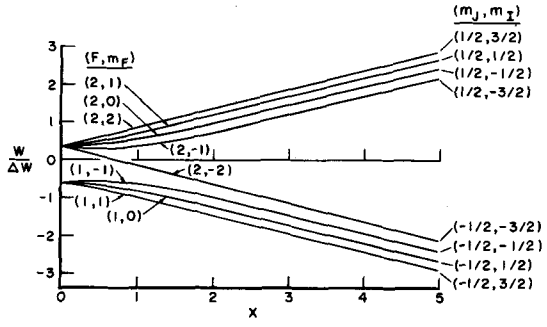

Fig. 7 - Energy diagram of the hyperfine structure levels of the ground state of potassium in a magnetic field. W = energy in units of the hyperfine structure splitting ΔW; $x = (g_J - g_I)\,\mu_o H/\Delta W$ in which g_J and g_I are the electron and nuclear g-factors, μ_o is the Bohr magneton, and H is the magnetic field. (F,m_F) are the weak field quantum numbers for total atomic angular momentum and its z component and (m_J, m_I) are the strong field quantum numbers for the z components of electronic and nuclear spins.

radiofrequency power is required with the simple induced transition.

The principle of adiabatic passage allows for the complete reversal in direction of a magnetic moment by a method which involves sweeping slowly the value of a quasi-static magnetic field in the presence of a radiofrequency field through the resonance value (27). If the rate of change of the quasi-static magnetic field is slow enough to satisfy the adiabatic condition, and if the magnitude of the change is large compared to the resonance line width, then a complete reversal in direction of the magnetic moment is achieved. Specifically (24), consider that atoms in the state 2 are to be transferred to the state 4. The quasi-static magnetic field is designated $H_o(t)$ and is the field seen by an atom moving through a region in which the field varies with position. The radiofrequency field is $H_1 \cos \omega t$ and is parallel to H_o. The resonance condition is $\omega = (E_2 - E_4)/\hbar$. The adiabatic condition requires that the quasi-static magnetic field H_o should vary monotonically in space along the atom's trajectory from a value below resonance to a value above resonance so that

$$\frac{d}{dt}\frac{(E_2 - E_4)}{\hbar} \simeq \frac{\Delta (E_2 - E_4)}{\hbar\, \Delta x}\frac{dx}{dt} \ll \mu_o^2 H_1^2/\hbar^2$$

in which $\Delta(E_2 - E_4) = \hbar\omega(H_o(\text{out})) - \hbar\omega(H_o(\text{in}))$ where H_o(in) and H_o(out) are the static magnetic field values at the entrance and exit points of the atom for the r.f. region, dx/dt is the atom velocity, Δx is the length of the r.f. region traversed by the atom, and μ_o is the Bohr magneton. The

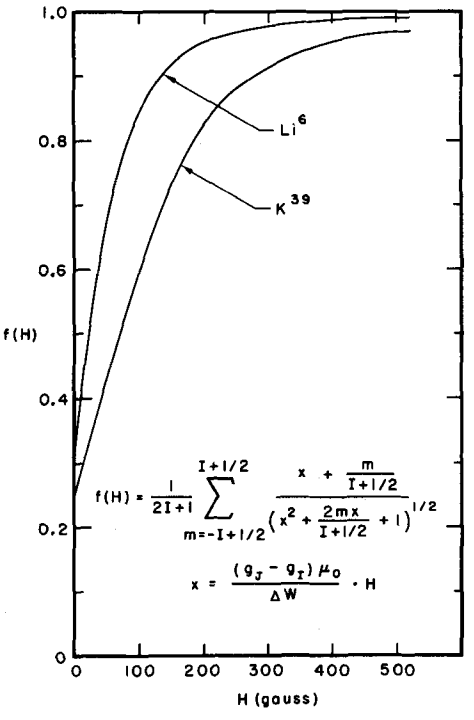

Fig. 8 - Electronic polarization, f(H), of potassium versus magnetic field for the group of saes having $m_j = +1/2$ in a strong magnetic field.

total change in H_o over the region must be such that

$$\Delta\omega = \Delta (E_2 - E_4)/\hbar \gg \mu_o H/\hbar$$

is satisfied. Typical values are $H_o = 1000$ G, H_o(out) − H_o(in) = 10 G, $f = \omega/2\pi \simeq 3000$ Mc/sec, Δx = 3 cm, $dx/dt = 3 \times 10^5$ cm/sec, and $H_1 = 1$ G.

Under this condition of strong H_o field atoms in states 1 and 4 will have a proton polarization close to 1. Ionization can then be accomplished in the relatively high magnetic field of 1000 G which facilitates the design of an electron gun with a high electron current and hence high ionization efficiency. Transitions can also be induced by the adiabatic method under weak field conditions and ionization can be accomplished in a strong magnetic field.

Transitions of atoms from the state 2 to the state 4 can also be induced by a simple resonance transition (26) in a homogeneous field H_o and a radiofrequency field $H_1\rho \cos \omega t$ where $\omega = (E_2 - E_4)/\hbar$ and $\mu_o H_1 \Delta T \simeq h/4$. If the time ΔT spent in the r.f. region is 10^{-5} sec, H_1 is approximately 0.01 G and hence considerably smaller than the value required in the adiabatic method. However, the requirements on stability of the frequency and amplitude of the r.f. field are more stringent for the simple induced transition. Under a strong H_o field condition the proton polarization after the resonance transition will be 0.76.

A schematic diagram of a polarized ion source is shown in Fig. 4. The principal operating pa-

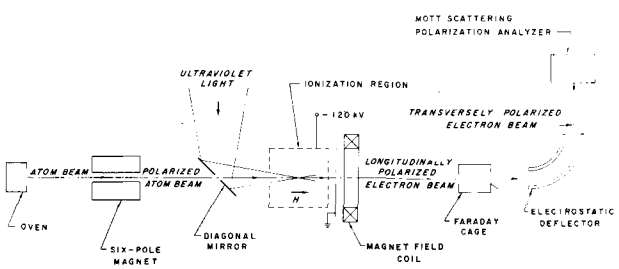

Fig. 9 - Schematic diagram of the polarized electron source and the arrangements for measuring current and polarization (not to scale).

rameters of a polarized proton ion source which represent the current state of the art are given in Table II.

The design of a polarized deuteron source is essentially the same as that of a polarized proton source. The energy level diagram for a deuterium atom in a magnetic field and the magnetic moments of the hyperfine states of deuterium are shown in Figs. 5 and 6, respectively. Because the spin of the deuteron is 1 a polarization tensor of 2nd rank must be considered (28). Without the use of an r.f. transition the value for the polarization tensor component $P_{33} = P_3$ of 0.30 can be achieved. With the use of a radiofrequency transition by the adiabatic passage method from state 3 to 6 the value for P_{33} can be increased to 0.60. The same beam intensities can be achieved as for proton sources.

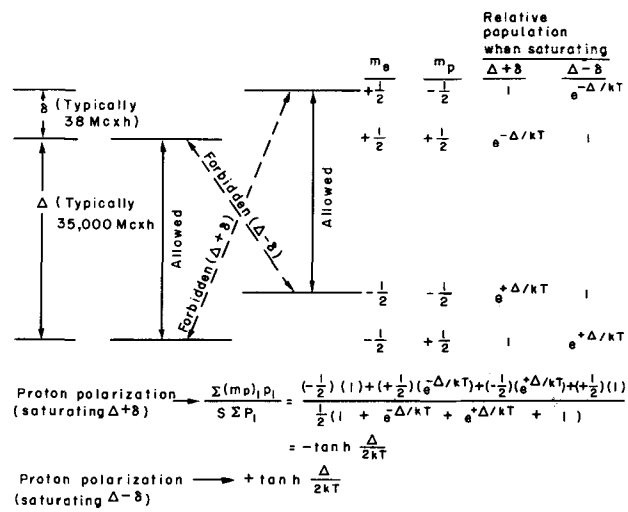

Fig. 10 - Energy level diagram for system of a paramagnetic center weakly coupled to a neighboring nucleus in an external magnetic field. The frequencies quoted are those appropriate for producing dynamic proton polarization in a lanthanum magnesium nitrate crystal with neodymium doping in a field of 9.1 kG.

A polarized ion source of He^3 can also be obtained by the atomic beam method. In its ground state the helium atom is in a $^1S_0$ state and hence the electronic magnetic moment is zero. For He^3 the nuclear spin I is 1/2. Deflection in the inhomogeneous magnetic field is achieved through the force on the nuclear magnetic moment. The nuclear polarization of the selected He^3 atoms will be close to 1. No polarized He^3 source has yet been reported but its intensity may be expected (29) to be of the same order of magnitude as that of polarized proton sources despite the smallness of a nuclear moment compared to an atomic moment because of the possibility of using a very low temperature beam of He^3 atoms.

It has recently been observed that quite high

TABLE II

Intensity of polarized proton ion source

Flux from oven source (1200 capillaries each 2 mm in length and ≃ 0.13 mm inside diameter; pressure ≃ 0.2 mm of Hg)	10^{19} sec
Fraction of atoms in $m_J = +1/2$ states accepted and transmited by magnet	2.2×10^{-3}
Fraction of atoms in $m_J = +1/2$ states	0.5
Flux of polarized atoms to ionizer (after r.f. transition region)	1×10^{16} sec
Ionization efficiency	3×10^{-3}
Flux of polarized protons	3×10^{13} sec (5μA)
Polarization	0.95

intensities of hydrogen atoms in the 2S metastable state can be formed in the reaction $H^+ + + Cs \rightarrow H(2S) + Cs^+$ for incident proton energies of about 1 keV (30). Since polarization of 2S hydrogen atoms can be accomplished with static and radiofrequency fields (31), such beams might prove useful in the future for polarized ion sources (2).

For use in a high energy accelerator a pulsed source of polarized ions is required. Inherently the atomic beam polarized ion sources are continuous sources, so the time average beam intensity for injection into a high energy accelerator is less than the source intensity by the acceptance duty factor of the accelerator. Thus, for example, if we consider the present operating conditions of the AGS at the Brookhaven National Laboratory, the injection time for five turn injection is 40 μsec and the repetition rate of the accelerator is 0.4/sec. Hence the duty factor is 1.7×10^{-5}. In addition we must consider the matching of the emittance of the polarized ion source to the acceptance of the proton linear accelerator injector and the effective phase acceptance factor of the linear accelerator. The matching factor can be taken equal to 1 and the phase acceptance factor can be taken as 0.5. Hence the overall reduction factor in intensity for the AGS is 0.8×10^{-5}. Hence if the polarized ion source has a continuous intensity of 5μA as indicated in Table II, the polarized proton intensity from the AGS will be 1.2×10^9 protons per pulse.

2. Acceleration of polarized particles (32)

Loss of polarization of a charged particle can occur in the acceleration process due to magnetic forces on the spin magnetic moment of the particle. The equation of motion of the spin vector $\vec{\sigma}$ of a charged particle in a magnetic field in the laboratory coordinate system can be written in the form (33):

$$\frac{d\vec{\sigma}}{dt} = \frac{e}{m_o c \gamma} \vec{\sigma} \times \left[(1 + \gamma G) \vec{B}_\perp + (1 + G) \vec{B}_\parallel \right]$$

in which $\vec{\sigma}$ is the spin vector, γ is the ratio of the particle energy to its rest energy $m_o c^2$, e is the particle's charge, $\vec{B}_\perp$, $\vec{B}_\parallel$ are the components of the magnetic field which are perpendicular and parallel to the particle's velocity, t is the time, and $G = (g/2) - 1$ is the anomalous magnetic moment coefficient. The appearance of γ indicates that the ratio of the spin precession frequency to the cyclotron frequency is anisotropic, i. e., depends upon the relative orientation of the magnetic field and the particle's velocity. For transverse fields the ratio increases with increasing energy, and this implies that at various energies the frequency of spin precession equals the frequency of some component of a depolarizing field, and when that occurs, we may obtain resonant depolarization.

Proton linear accelerators of the Alvarez type have been successfully used to accelerate longitudinally or transversely polarized protons to energies of about 60 MeV without appreciable loss in polarization (22, 34). It is expected that acceleration to higher energies in linear accelerators will also maintain the proton polarization, although explicit calculations of depolarization in high energy linear accelerators have not been published.

For circular accelerators the protons are constrained to move in circles by a primary magnetic guide field and are subjected to perturbing fields associated with field-free straight sections radiofrequency acceleration, magnet imperfections, and the betatron oscillations (principally the vertical one) of the protons. Resonances for spin motion occur when

$$\gamma G = k P \pm \nu \quad \text{(intrinsic)}$$

$$\gamma G = k \quad \text{(imperfection)}$$

in which k = an integer, P = number of identical periods in the magnet structure and ν is the vertical betatron oscillation frequency in units of the cyclotron frequency. The so-called intrinsic resonances are associated with vertical free oscillations about the equilibrium orbit and the imperfection resonances are associated with vertical displacements of the equilibrium orbit due to magnet imperfections.

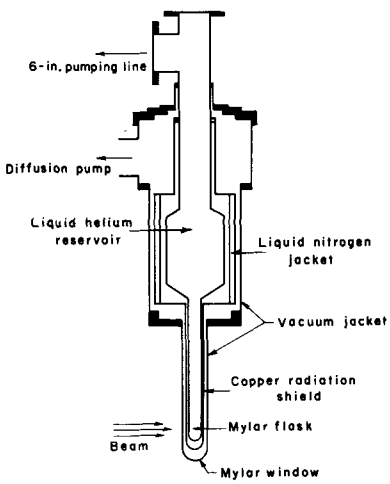

Fig. 11 - Cryostat used to maintain Berkeley polarized proton target at 1.2 °K.

The orbit dynamics of the particular accelerator determines the relative importance of the different possible resonances. In a cyclotron or a synchrotron without straight sections, P is infinite so that only the imperfection resonances occur. The resonance with $k = 2$ occurs at 110 MeV and may lead to depolarization if the second harmonic component of the magnetic field in the mediant plane is not small (35, 36). In sector-focused cyclotrons the intrinsic resonances are the principal ones (37), since P is finite and in practice may have the values 3, 4, 6, or 8. In weak-focusing synchrotrons the intrinsic resonances $\gamma G = P \pm \nu$ are most troublesome. In strong-focusing synchrotrons such as the AGS at the Brookhaven National Laboratory, the principal resonance occurs at $\gamma G = \nu$.

The energies at which the principal resonances occur for some existing high energy accelerators are given in Table III. The strength of a resonance depends on the rate of acceleration and on the amplitude of the betatron oscillations, so that high acceleration rates and well-collimated beams favor acceleration without depolarization. Schemes to avoid resonant depolarization can be imagined; for example, additional magnets along the orbit might be used to change the betatron frequency rapidly as each resonance is approached.

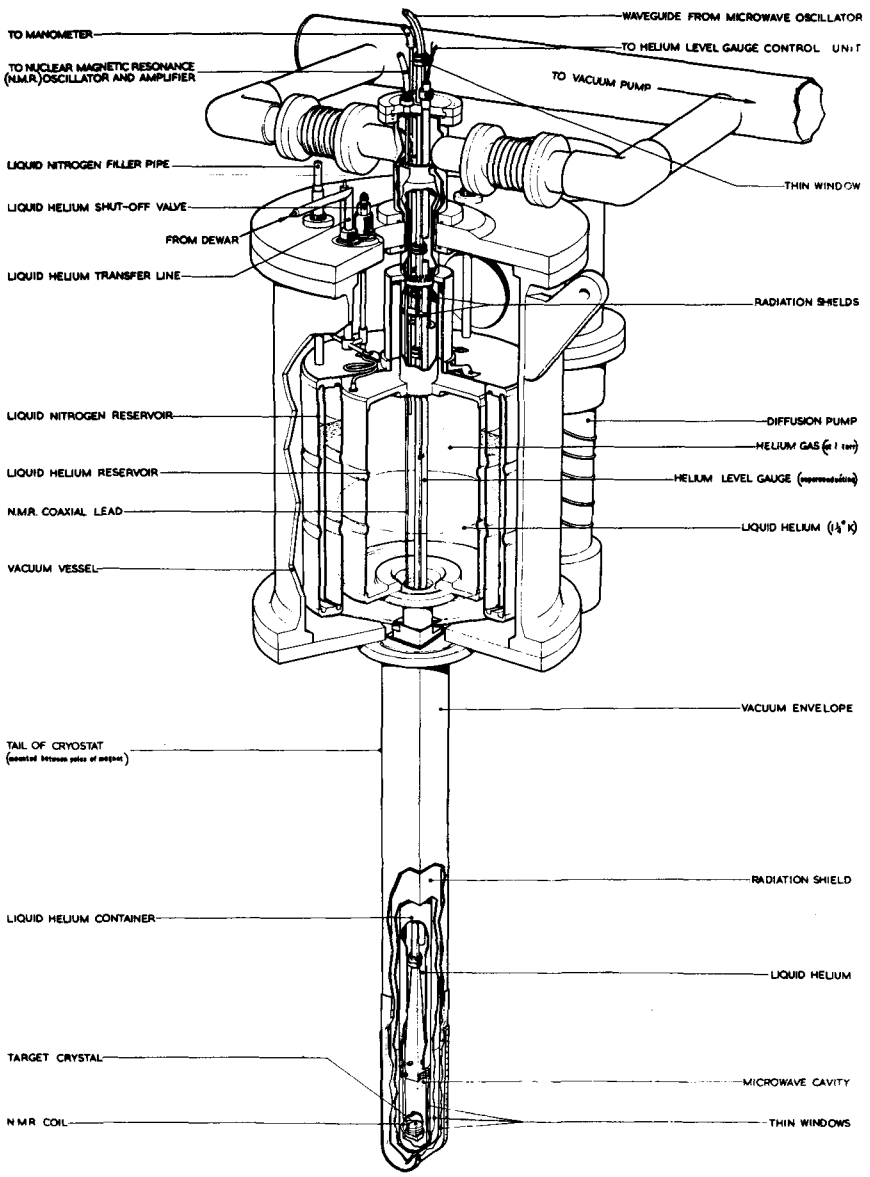

DETAILS OF CRYOSTAT

Fig. 12 - Diagram of Rutherford polarized proton target.

3. Sources of polarized electrons

A source of polarized electrons based on the atomic beam technique and involving the photoionization of polarized alkali atoms has recently been developed (38, 39). The energy level diagram for the ground state of potassium in a magnetic field is shown in Fig. 7. Atoms with the electronic magnetic quantum number $m_J = +1/2$ are selected by deflection in a strong inhomogeneus magnetic field provided by a six-pole magnet. The selected atoms having an electron polarization P_a close to unity enter the photoionization region where there is a weaker magnetic field H along the axis of propagation. They change adiabatically into the states characteristic of H for which the electronic polarization P is smaller than P_a due to the hfs coupling of the electronic spin and the nuclear spin I:

$$P = P_a f(H)$$

The quantity f(H) is given in Fig. 8, and is plotted for K^{39} and Li^6. Photoionization is predominantly an electric dipole transition and hence the polarization of the photoelectrons should be equal to the electronic polarization P of the atoms. Potassium was chosen as the alkali atom because of its relatively small hfs interaction and relatively low photoionization threshold energy corresponding to $\lambda = 2856$ Å.

A schematic diagram of the polarized electron source and of the Mott scattering apparatus used to measure the electron polarization is shown in Fig. 9. The inhomogeneous magnetic field is provided by a six-pole magnet and the light source is a high pressure mercury arc. Photoionization occurs in the region between two cylindrical electrodes with a small bias voltage between them suitable for electron extraction and with the electrodes at about -120 kV, in order that the analysis of the electron polarization can be made by the Mott scattering method. The axial magnetic field is 90 G. For measurement of the electron polarization the electron beam is passed through a 112° cylindrical electrostatic deflector, which converts the longitudinal polarization into a transverse polarization, and then scattered in a gold foil.

A value for the electron polarization P of 0.58 ± 0.03 was measured, in good agreement with the expected polarization for H = 90 G of $P = P_a f(H) = (0.96)(0.58) = 0.56$. The current was $\sim 10^{-12}$ A or 6×10^6 sec. The operating characteristics are given in Table IV. Both the electron polarization and current do not represent the ultimate capacities of this method. An electron polarization of at least 0.9 can be expected with higher magnetic fields and increase in the photoionization efficiency, which should be possible, will increase the current.

We now give estimates (Table V) on a pulsed source of polarized electrons for a high energy electron linear accelerator (specifically we consider the Stanford Mark III 1 BeV electron linear accelerator). The use of a lithium atomic beam appears promising. The photoionization cross section for lithium is about 200 times greater than that of potassium and although the threshold wavelength for photoionization is lower (2300 Å), under pulsed operation the high pressure spark provides a flash lamp of high radiance in the wavelength range from 2300 Å to 1800 Å (the lower limit of quartz optics). The isotope Li^6 has a small hfs interval $\Delta\nu = 228$ Mc/sec and hence an ionizing field of 200 G results in an electron polarization of 0.95. Table V indicates the conditions for photoionization and the resulting current of polarized electrons.

Electron beams with a polarization of 0.8 have been produced by scattering electrons of about 1 keV energy by mercury atoms (40). Experimental results (41) are in agreement with the Mott theory of scattering by the screened and unscreened Coulomb field (42). As yet a beam intensity of only 10^{-13} amp has been obtained

TABLE III

Conditions for resonant depolarization

Accelerator	γG	E (kinetic) BeV
Cosmotron or Saturne	$4 - \nu = 3.2$	0.74
	$4 + \nu = 3.8$	1.1
Princeton-Penn	$8 - \nu = 7.1$	2.8
Argonne (ZGS)	$8 - \nu = 7.1$	2.8
	$8 + \nu = 8.9$	3.8
Brookhaven AGS	$12 - \nu = 3.25$	0.76
	$\nu = 8.75$	3.6
CERN PS	$10 - \nu = 3.75$	1.0
	$\nu = 6.25$	2.3

TABLE IV

Intensity of polarized electron source achieved with potassium atomic beam

Flux from oven source	5×10^{17} sec
Fraction of atoms in $m_J = +1/2$ states accepted and transmitted by magnet	4×10^{-4}
Fraction in $m_J = +1/2$ states	0.5
Flux of polarized atoms to photoionization region	1.2×10^{14} sec
Photoionization efficiency	5×10^{-8}
Flux of polarized electrons	6×10^6 sec
Electronic polarization (at high fields)	0.97

TABLE V

Pulsed source of polarized electrons for high energy linear accelerator
(Design Parameters)

Light source: high-pressure spark	Flash duration, 1 μs; energy 1 joule/flash with 5% emitted in useful wavelength range; luminous area, 2×2 mm²; 60 pulses per sec
Optics	Useful light solid angle at spark, 1.8 sr; lateral magnification, 3 times to coincide with atomic beam cross section; total absorption and reflection losses, 50%; average photon-atom interaction length, 1 cm
Photoionization efficiency	About 3% of the Li atoms in 1 cm beam length will be ionized
Lithium atomic beam	Atom density, 4×10^9 cm^{-3}; beam cross section, 7 mm diam
Polarized electron source	Intensity, 3×10^7 electrons/pulse; electron polarization greater than 0.9
High energy beam of polarized electrons	Intensity, 3×10^6 electrons/pulse with assumption of 10% transmission by 1 BeV Stanford linear accelerator; polarization greater than 0.9

due in part to the necessity to avoid plural scattering, but higher beam intensities can be anticipated.

No loss in electron polarization is expected in the linear accelerator; however successful acceleration of polarized electrons or positrons has not yet been demonstrated (43). Resonant depolarization in strong-focusing electron synchrotrons (CEA and DESY) can occur as it does for the proton accelerators. For the 6 BeV Cambridge Electron Accelerator which has $\nu = 6.4$, the principal intrinsic resonance occurs at 2.8 BeV and the first imperfection resonance occurs at 440 MeV. Numerical calculations have been reported (44) which are relevant to the Yerevan electron synchrotron.

A high energy beam of polarized muons will be provided in the muon storage ring designed for use with the CERN PS (45). The polarization results from parity nonconservation in the pion decay. High energy electrons and positrons in storage rings may become polarized through the process of synchrotron radiation (46).

C - POLARIZED TARGETS

1. Polarized protons

Polarized photon targets based on dynamic nuclear orientation and utilizing as the target a crystal of $La_2Mg_3(NO_3)_{12}\cdot 24\,H_2O$ doped with Nd are now in active use in several laboratories. There have been a number of excellent discus-

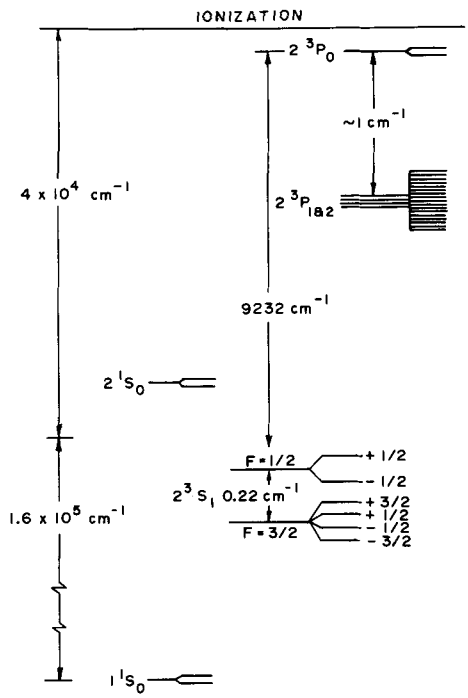

Fig. 13 - Energy levels of He^3 atom in external magnetic field (not to scale).

sions (47, 48, 49) of the basic principles and operating characteristics of this target. Hence we will only review the subject here briefly following the discussion in Shapiro's article (49).

The system consists of electrons with spin S (provided by the magnetically dilute paramagnetic Nd ions), and protons with spin I (provided by the H atoms). The energy levels of one electron and one proton in a strong magnetic field are shown in Fig. 10 and are given by

$$E = m_e \Delta - m_p \delta$$

in which m_e and m_p are the magnetic quantum numbers of the electron and proton, respectively, $\Delta = g_e\mu_o H$ and $\delta = g_p\mu_o H$ where g_e and g_p are theelectron and proton g-values, μ_o is the Bohr magneton and H is the magnetic field. There is a magnetic dipole-dipole coupling between the electron and proton. This coupling is sufficiently small so that its effect on the energy levels can be neglected but it causes a small but significant change in the eigenfunctions so that they are not pure eigenstates for the spin projection operators. Thus the state which in the absence of the magnetic dipole-dipole interaction would have $m_e = +1/2$ actually has a small admixture of $m_e = -1/2$ eigenstate as well, and viceversa. With only the static magnetic field present and under low temperature conditions the proton polarization,

$p = < I_z > /I$, for the system in thermal equilibrium will be

$$p \simeq \frac{-1}{4}\left(\frac{\Delta}{kT}\right)\left(\frac{\delta}{(kT}\right)$$

which in practice is a small number.

Dynamic nuclear orientation involves inducing a so-called forbidden transition and thus achieves a high proton polarization. Thus referring to Fig. 10, if the states were pure eigenstates of m_e and m_p, there would be no matrix element of the interaction Hamiltonian term involving the r.f. magnetic field between the states designated by $(m_e, m_p) = (-1/2, +1/2)$ and $(+1/2, -1/2)$; however due to the eigenstate admixture arising from the magnetic dipole-dipole interaction this transition involving both a proton and electron spin flip can be saturated with sufficiently high r.f. power so that the population of these two levels is equalized. We assume that the pairs of levels $(m_e, m_p) = (-1/2, +1/2), (+1/2, +1/2)$ and $(-1/2, -1/2), (+1/2, -1/2)$, for which the allowed selection rule $\Delta m_e = +1, \Delta m_p = 0$ applies, are maintained in thermal equilibrium by the electron spin-lattice relaxation. Relaxation mechanisms are assumed to be unimportant between

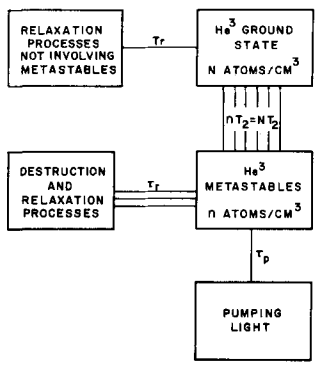

Fig. 14 - Schematic diagram indicating the interactions determining the polarizations of metastable and ground state He^3 atoms.

levels for which $\Delta m_p = \pm 1$. Under these conditions the level populations are indicated in Fig. 10 and the proton polarization will be

$$p = -\tanh\frac{\Delta}{2kT} \simeq \frac{-\Delta}{2kT}$$

which in practice can be close to 1. If instead the other forbidden transition $(m_e, m_p) = (-1/2, -1/2) \leftrightarrow (+1/2, +1/2)$ is saturated, then the proton polarization will have the opposite sign.

$$p = +\tanh\frac{\Delta}{2kT} \simeq \frac{+\Delta}{2kT}$$

Several practical targets have been described recently (50, 51). Proton polarizations as high as 70-80% are achieved and target masses are up to 30 gms with hydrogen being 3% by weight.

Figs. 11 and 12 show the Berkeley (49) and Rutherford (51) targets.

2. Polarized deuterons

The same scheme of dynamic nuclear orientation which was discussed for protons in the previous section has been used recently (52) for deuterons as well with a targeto of $La_2Mg_3(NO_3)_{12} \cdot 24\ D_2O$. Because of the relative smallness of the deuteron magnetic moment compared to the proton magnetic moment, a polarization of less than 10% is achieved.

The method of dynamic nuclear orientation has been applied to solid deuterium containing trapped deuterium atoms (53). The samples were grown by passing gaseous deuterium through an electrode less r.f. discharge and condensing the products into a microwave cavity maintained at 1.2 °K by a bath of liquid helium. In solid deuterium the majority of the molecules will be in the orthostate and hence the nuclear spin of the molecule will be $I = 2$. Deuterium atoms in this solid matrix serve as paramagnetic centers with electronic spin $S = 1/2$. If this system is placed in a strong magnetic field, an energy level diagram analogous to but somewhat more complicated than that of Fig. 10 for protons is obtained. Because of the magnetic dipole-dipole coupling between the orthodeuterium spin and the electronic spin of the deuterium atom a so-called forbidden transition involving a change in both the nuclear spin orientation and the electronic spin orientation can be induced and indeed saturated with high microwave power at the resonant frequency. The resulting polarization of the deuterium nuclei is carried throughout the sample by nuclear spin diffusion. If the nuclear spin-lattice relaxation time is small (54), high deuteron polarization can be obtained in principle.

Thus far an increase in the deuteron polarization due to the r.f. by a factor of 70 at T = 1.2 °K has been achieved and corresponds to a polarization of 1.1%. Much higher polarizations can be expected if greater densities of deuterium atoms can be achieved in the solid lattice (55).

3. Polarized helium-3

Since the nucleus He^3 has its two protons in opposite spin states so that the net spin and ma-

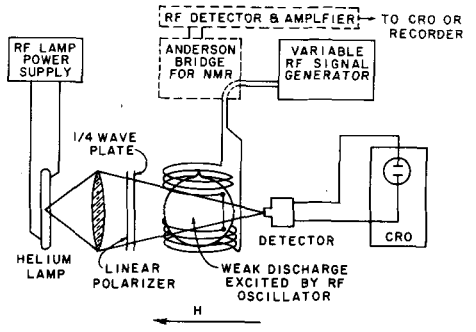

Fig. 15 - Schematic diagram of equipment used in performing resonance experiments on optically pumped He^3.

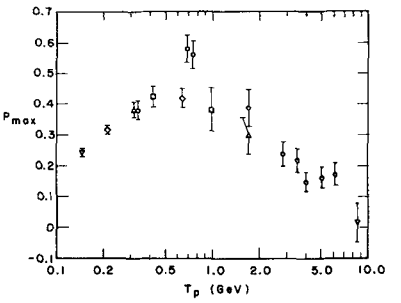

Fig. 17 - Maximum polarization as a function of beam energy T_p. O, data from Berkeley experiment with polarized proton target. Other points involved data from double scattering experiments.

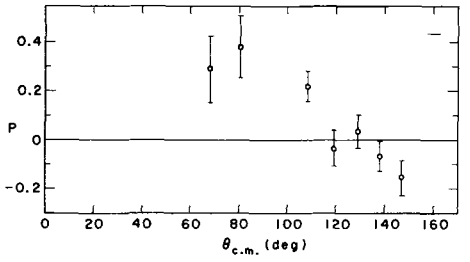

Fig. 16 - The polarization parameter P in elastic pion-proton scattering at 246 MeV pion kinetic energy.

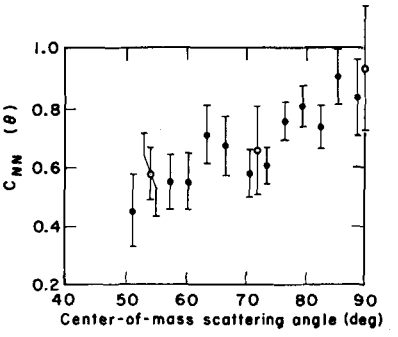

Fig. 18 - $C_{NN}(\theta)$ in elastic proton-proton scattering at 680 MeV. (The open circles are from triple scattering experiments by Golovin et al: Soviet Physics - JETP 17, 98 (1963).

gnetic moment are simply those of a neutron to an excellent approximation, a polarized He^3 target may be regarded as some approximation to a target of polarized neutrons from the viewpoint of high energy physics.

A gas target of polarized He^3 nuclei has been produced by the method of optical pumping (56). Fig. 13 shows the energy level diagram of He. Ground state He^3 atoms are excited to the metastable $2\,^3S_1$ state by a weak discharge. A He lamp is used together with a polarizer to excite atoms to the $^3P_0$ state in $\Delta m = +1$ transitions. From the short-lived (10^{-7} second) $^3P_0$ state atoms decay to all the $^3S_1$ state magnetic sublevels. The net result is a transfer of atoms from sublevels of low magnetic quantum number ($m = -3/2, -1/2$) to those with higher magnetic quantum number $m = +1/2, +3/2$, or equivalently a transfer of angular momentum from the polarized light to the atoms. The metastable atom (He^{3*}) polarization is then transferred to ground state He^3 atoms as nuclear polarization via the metastability exchange collisions:

$$He^3 + He^{3*} \rightarrow He^{3*} + He^3$$

which can occur with sipn flip. Fig. 14 is a schematic diagram of the interactions and Fig. 15 is a schematic diagram of the equipment.

Nuclear polarizations of He^3 as high as 40% have been achieved. Typically the gas sample has a volume of 65 cm^3 at a pressure of 1 mm of Hg. At higher pressures the nuclear polarization is small, possibly due to inefficiency of the discharge and to increased effectiveness of processes which destroy the metastable atoms. Since the relaxation time for the He^3 ground state polarization is long (~ 4000 sec), it may be possible to compress and store the polarized He^3 atoms. Although the target density achieved so far is small, low energy nuclear scattering experiments have been done with this target (57).

D - HIGH ENERGY EXPERIMENTS WITH POLARIZED TARGETS

The only high energy experiments with polarized particles reported thus far have been those which

have used the polarized proton target based on the dynamic nuclear polarization method and using crystals of $La_2Mg_3(NO_3)_{12} \cdot 24H_2O$ doped with Nd. The experiments have been measurements of π-p and p-p elastic scattering with a polarized proton target.

The first high energy experiment was done at Berkeley by Chamberlain, Jeffries, Schultz and Shapiro on the scattering of 250 MeV π^+ mesons on polarized protons (59). Substantial left-right asymmetries were observed and the polarization parameter P was measured. (See Fig. 16). It is clear that the P values are relatively large and hence important to the determination of the scattering matrix.

Several experiments have been reported by the Beckeley group on proton-proton scattering using a polarized proton target (60). Measurements were made of the polarization parameter, P, which is defined according to

$$\left.\frac{d\sigma}{d\Omega}\right|_{pol} = \left.\frac{d\sigma}{d\Omega}\right|_{unpol} (1 + P(\theta) P_T)$$

where P_T is the target polarization. Results for $P(\vartheta)_{max}$ in the energy range from 0.33 to 6.15 BeV are shown in Fig. 17. The correlation parameter C_{NN} was measured from the scattering of a polarized proton beam, obtained in a first scattering, from a polarized proton target (61). The results are shown in Fig. 18.

Recently work has been reported both from the Rutherford laboratory (62) and the Argonne National Laboratory (63) on pion-proton scattering using a polarized proton target. The polarization in $\pi^- + p$ elastic scattering at 2.08 BeV/c has been measured at the ZGS with the results shown in Fig. 19. These measurements show that the usual assumption of a single scalar amplitude to describe elastic scattering in this energy region is not valid. At the Rutherford laboratory polarization measurements in $\pi^- + p$ elastic scattering were made in the momentum

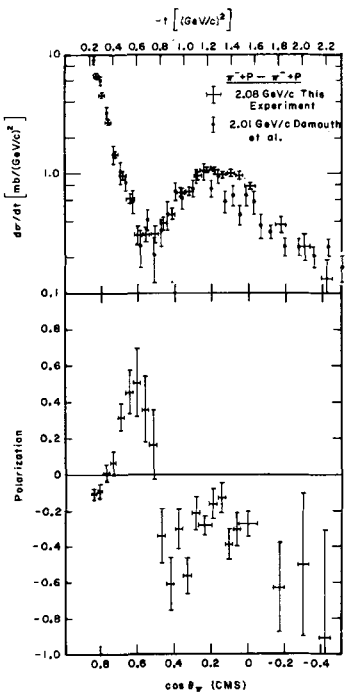

Fig. 19 - Experimental results at 2.08 BeV/c from ZGS experiment.
a) Differential cross section against cos ϑ_π (CMS). A scale of -t is also shown.
b) Polarization P. Vertical bars indicate statistical errors; horizontal bars represent the angular resolution. The normalization errors on the differential cross section and on P are $\pm$ 5% and $\pm$ 16%, respectively.

range from 875 to 1579 MeV/c and the conclusions deduced were that the resonances at 1030 MeV/c and 1480 MeV/c are F-wave resonances with $J = 5/2$ and $J = 7/2$ respectively.

At CERN a determination of the parity of the Ξ particle is being made using a polarized proton target (64).

In conclusion, the basic techniques for the development of useful polarized targets and polarized beams for high energy physics are either available or clearly in sight. The realization of accelerated beams of polarized particles will require at this stage the more active participation of accelerator physicists. Polarized beams and polarized targets will make possible a large number of important experiments which are either very difficult or essentially impossible with other presently known techniques. It is quite certain that as high energy and elementary particle physics become more sophisticated knowledge and control of the spin variable will be valuable.

REFERENCES

(1) J. M. Daniels: Oriented Nuclei, Polarized Targets and Beams, Academic Press, New York, 1965.
(2) International Conference on Polarization Phenomena of Nucleons, Karlsruhe, September 1965.
(3) T. D. Lee and C. N. Yang: Phys. Rev. *104*, 254 (1956).
(4) D. H. Wilkinson: Phys. Rev. *109*, 1603 (1958); Yu. G. Abov, P. A. Krupchitsky and Yu. A. Oratousky: Phys. Letters *12*, 25 (1964); F. Boehm and E. Kankeleit: Phys. Rev. Letters *14*, 312 (1965); R. E. Segel, J. W. Olness and E. L. Sprenkel: Phys. Rev. *123*, 1382 (1961); International Conference on Polarization Phenomena of Nucleons, Karlsruhe September 1965; M. Forte and D. Saavedra: Investigation of Parity Nonconservation Effects in the Radiative Capture of Polarized Neutrons. The case of H^2 (n, γ) and Cd^{113} (n, γ).
(5) C. W. Drake, D. C. Bonar, R. D. Headrick, and V. W. Hughes: Parity Conservation in Strong Interactions, International Conference on Polarization Phenomena of Nucleons, Karlsruhe, September 1965.

(6) L. Wolfenstein: Annual Review of Nuclear Science (Annual Reviews, Inc., Palo Alto, 1956) Vol. 6, p. 43.
(7) E. H. Thorndike: Phys. Rev. *138*, B586 (1965).
(8) L. Rosen and J. E. Brolley, Jr.: Phys. Rev. Letters *2*, 93 (1959); D. Bodansky, S. F. Eccles, G. W. Farwell, M. E. Rickey, and P. C. Robinson: Phys. Rev. Letters 2, 101 (1959); E. M. Henley and B. A. Jacobsohn: Phys. Rev. *113*, 225 (1959).
(9) *Collision Theory*, Marvin L. Goldberger and Kenneth M. Watson, (John Wiley and Sons, Inc., 1964).
10) The Present Status of Very High Energy $\bar{p}-p$, $\pi^{\pm}-p$ and $K^{\pm}-p$ Scattering, S. J. Lindenbaum. Presented at the Second Coral Gables Conference on Symmetry Principles at High Energy, January 20-22, 1965.
(11) G. Breit: Encyclopedia of Physics, XLI/1 (Springer, Berlin, 1959).
(12) Interactions of Pions and Nucleons above 1 GeV/c, S. J. Lindenbaum, August 1964, Dubna Conference on High Energy Physics, 1964.
(13) *Nucleon Structure*, Edited by R. Hofstadter and L. I. Schiff, Stanford University Press, Stanford, California (1964). D. R. Yennie, p. 11.
(14) L. Durand, III, Reference 13, p. 28.
(15) C. K. Iddings: Phys. Rev. *138*, B446 (1965).
(16) W. E. Cleland, J. M. Bailey, M. Eckhause, V. W. Hughes, R. M. Mobley, R. Prepost and J. E. Rothberg, Phys. Rev. Letters *13*, 202 (1964).
(17) W. Zickendraht, D. J. Andrews ,and M.L. Rustgi, Phys. Rev. Letters 7, 252 (1961).
(18) S. M. Bilenky: Il Nuovo Cimento *10*, 1049 (1958).
(19) S. M. Bilenky and R. M. Ryndin: Phys. Letters *18*, 346 (1965).
(20) L. J. B. Goldfarb and D. A. Bromley; Phys. Rev. Letters *9*, 106 (1962). A relevant discussion for nuclear physics reaction studies is given.
(21) S. Barshay: Phys. Letters *3*, 320 (1963); S. M. Berman: Phys. Rev. *135*, B1249 (1964); M. J. Moravcsik, Pyhs. Rev. *125*, 1088 (1962).
(22) J. M. Dickson: Polarized Ion Sources and the Acceleration of Polarized Beams. Progress in Nuclear Techniques and Instrumentation, Vol. 1, ed. F.J. M. Farley, 1964.
(23) Proceedings of the International Symposium on Polarization Phenomena of Nucleons, Basel, July 4-8, 1960. Editors: P. Huber and H. P. Meyer, Helv. Phys. Acta Supp. VI, 1961 (Birkhauser Verlag Basel und Stuttgart).
(24) A. Abragam and J. M. Winter: Phys. Rev. Letters *1*, 374 (1958).
(25) V. W. Hughes, C. W. Drake, Jr., D. C. Bonar, J. S. Greenberg and G. F. Pieper: See reference 23; C. W. Drake, D. C. Bonar, R. D. Headrick and V. W. Hughes: 1961 Proceedings of International Conference on High Energy Accelerators, p. 379 1961) and Rev. Sci. Instr. 32, 995 (1961).
(26) P. Kusch and V. W. Hughes: Encyclopedia of Physics (Springer-Berlin, 1959).
(27) A. Abragam: The Principles of Nuclear Magnetism, Oxford, Clarendon Press, 1961, p. 34.
(28) L. J. B. Goldfarb: Nucl. Phys. 7, 622 (1958); S. Devons and L. J. B. Goldfarb: Encyclopedia of Physics, XLII (Springer, Berlin, 1957), p. 362.
(29) M. K. Craddock: (private communication).
(30) B. L. Donnally, T. Clapp, W. Sawyer, and M. Schultz: Phys. Rev. Letters *12*, 502 (1964).
(31) W. E. Lamb and R. C. Retherford: Phys. Rev. *79*, 549 (1950).
(32) E. D. Courant: Acceleration of Polarized Protons to Relativistic Energies, BNL Internal Report, January 1962. Our discussion is essentially the treatment given in this BNL internal report.
(33) H. Mendlowitz and K. M. Case: Phys. Rev. *97*, 33 (1955); V. Bargmann, L. Michel, and V. L. Telegdi: Phys. Rev. Letters *2*, 435 (1959); R. Hagedorn: Relativistic Kinematics, W. A. Benjamin, Inc., New York (1963).
(34) D. Cohen and A. J. Burger: Rev. Sci. Instr. *30*, 1134 (1959).
(35) M. Froissart and R. Stora: Nucl. Instr. and Methods 7, 297 (1960).
(36) F. Lobkowicz and E. H. Thorndike: Rev. Sci. Instr. *33*, 434 (1962).
(37) T. K. Khoe and L. C. Teng: International Conference on Sector-Focused Cyclotrons and Meson Factories, CERN (1963), p. 118.
(38) R. L. Long, W. Raith and V. W. Hughes: Phys. Rev. Letters *15*, 1 (1965): V. W. Hughes, R. L. Long, Jr., M. Posner and W. Raith: International Symposium on Electron and Photon Interactions at High Energies, Hamburg, 1965.
(39) V. W. Hughes, R. L. Long and W. Raith: Proceedings of International Conference on High Energy Accelerators, Dubna, 1963, p. 988.
(40) K. Jost and J. Kessler: Phys. Rev. Letters *15*, 575 (1965).
(41) H. Deichsel and E. Reichert: Z. Physik *185*, 169 (1965), and earlier work; H. Steidl, E. Reichert and H. Deichsel: Phys. Letters *17*, 31 (1965).
(42) G. Holzwarth and H. J. Meister: Nucl. Phys. *59*, 56 (1964); P. J. Bunyan and J. L. Schonfelder: Proc. Phys. Soc. (London) *85*, 455 (1965).
(43) W. Chinowsky, D. Cutts, and R. Stiening: Il Nuovo Cimento *34*, 1431 (1964).
(44) Kh. A. Simonian: Numerical-Analytical Calculation of the Acceleration of Polarized Electrons in a Synchrotron, Paper presented to this conference, see Session X.
(45) J. M. Bailey, F. J. M. Farley et al.: First tests of the CERN muon storage ring. Paper presented to this conference, see Session X.
(46) V. N. Bayer, Ju. F. Orlov: Quantum depolarization of electrons in a magnetic field. Paper presented to this conference, see Session IX.
(47) A. Abragam and M. Borghini: Progress in Low Temperature Physics, Vol. 4, 1964 (Amsterdam, North-Holland Pub. Co.).
(48) C. D. Jeffries: Dynamic Nuclear Orientation (New York, John Wiley and Sons, Inc., 1963).
(49) G. Shapiro: Polarized Targets, Progr. in Nucl. Tech, and Instrumentation (Amsterdam, North-Holland Pub. Co., 1964).
(50) S. Suwa, A. Yokosawa, T. K. Khoe, A. Moretti: Performance of a Polarized Proton Target for High Energy Physics Experiments at Argonne. Preprint.

(51) H. H. Atkinson, B. E. Belcher, B. F. Colyer, and R. Downton: A. Polarized Proton Target for Nimrod. Paper presented to this Conference, see Session X.
(52) V. I. Lushchikov, Yu. V. Taran, and A. I. Frank: JETP Letters, *1*, 52, (1965).
(53) G. Rebka and M. Waine: Bull. Am. Phys. Soc. 7, 538 (1962); Polarization of Nuclei in Solid Deuterium by M. Waine, Yale University, PhD Thesis, 1965.
(54) M. Sharnoff and R. V. Pound: Phys. Rev. *132*, 1003 (1963).
(55) C. K. Jen, S. N. Foner, E. L. Cochran and V. A. Bowers: Phys. Rev. *112*, 1169 (1958).
(56) F. D. Colegrove, L. D. Schearer and G. K. Walters: Phys. Rev. *132*, 2561 (1963).
(57) G. C. Phillips, R. R. Perry, P. M. Windham, G. K. Walters, L. D. Schearer and F. D. Colegrove: Phys Rev. Letters *9*, 502 (1962).
(58) O. Chamberlain, C. D. Jeffries, C. H. Schultz, G. Shapiro and L. van Rossum: Phys. Letters 7, 293 (1963).
(59) C. H. Schultz: Scattering of 250 MeV positive pi mesons from a polarized proton target. Berkeley PhD thesis, 1964 UCRL-11149.
(60) O. Chamberlain et al.: Polarization in Proton-proton scattering using a polarized target. Proceedings of International Conference on High Energy Physics, Dubna, 1964; F. W. Betz: Polarization Parameter in Proton-Proton Scattering from 328 to 736 MeV, Berkeley PhD Thesis, 1964.
(61) H. E. Dost: Measurement of the Spin Correlation Parameter C_{nn} in Proton-Proton Scattering at 680 MeV. Berkeley PhD Thesis, 1965.
(62) Shigeki Suwa, Ahihiko Yokosawa, Norman E. Booth, Robert J. Esterling and Roger E. Hill, Phys. Rev. Letters *15*, 560 (1965).
(63) P. J. Duke, D. P. Jones, M. A. R. Kemp, P. G. Murphy, J. D. Prentice, J. J. Thresher, H. H. Atkinson, C. R. Cox and K. S. Heard: Phys. Rev. Letters *15*, 468 (1965).
(64) C. Rubbia: private communication.

RECENT PROGRESS IN THE PERFORMANCE OF ELECTROSTATIC SEPARATORS AT CERN

C. Germam

CERN, Geneva (Switzerland)

I. INTRODUCTION

This paper describes some advances in electrostatic separator techniques which have been made at CERN. A number of separators have been constructed and used in the proton synchrotron beam lines during the last four years. They comprise five large separators, each of which is 10 metres long, and which have previously been described in detail (1) and a further four, more recently constructed ones, each 3 metres in length. These 3 metre separators may be bolted together to form 6 metre units. In all these the magnetic field is deliberately separated from the electric field and localized in small compensating magnets placed at each end of the separator.

Considerable experience on the behaviour of these separators has been accumulated during the years and their operation under working conditions, with increasing reliability, in the beam lines of the CERN proton synchrotron, has been carried out by P. Coet and his team. The following shows the operating conditions currently achieved using our conventional stainless steel electrodes, provided organic vapour contamination is minimized: gap width 10 cm, applied voltage 550 to 600 kV; gap width 14 cm, applied voltage 700 to 740 kV.

In addition to the construction of operating units effort has also been directed in the N.P.A. Division to research on high voltage vacuum breakdown phenomena and to the development of separator technology. A search for improved electrodes has been made and it has been found (2) that by using a cathode coated with a thin insulating layer and a conventional stainless steel anode the performance of a 3 metre separator can be doubled. That is, the same voltage can be maintained across a gap of 5 cm instead of 10 cm (Fig. 1).

II. FABRICATION OF OXIDE COATED ALUMINIUM ELECTRODES

A number of different types of insulating cathode layers have been studied. The best re-